Supporting Information

Integrating Active C_3N_4 Moieties in Hydrogen-bonded Organic Frameworks for Efficient Photocatalysis

Tao Li, Bai-Tong Liu, Zhi-Bin Fang, Qi Yin, Rui Wang and Tian-Fu Liu *

Table of contents

1. Materials

Unless otherwise mentioned, all reagents and solvents were purchased from commercial sources and used as received without further purification.

2. Experimental section

2.1. Ligand Synthesis[1]

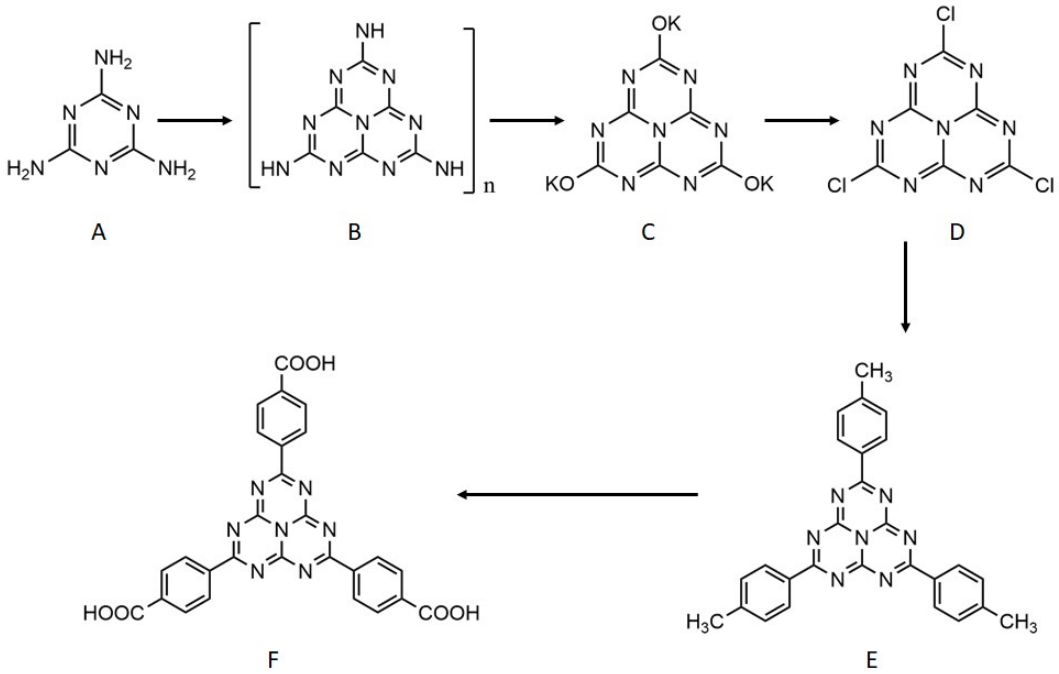

(1) Synthesis of B

50 g of melamine (2,4,6-triamino-*s*-triazine) was put into an evaporating dish and heated at about 300 °C for several hours until almost no gas came out. The white solid was then heated at 450 °C for 2 hours. The light yellow solid was washed with 100 mL 10% KOH aqueous solution and then boiled with 36% of HCl aqueous solution for 10 minutes to yield 25 g of melon. (25 g, yield: 50 %).

(2) Synthesis of C

25 g of melon (B) was refluxed with 500 mL of 2.5 M KOH aqueous solution until all the solids were dissolved. The solution was then concentrated to about 200 mL. A large number of white needle crystals appeared. The solution was cooled to 0 ℃ in the bath

of ice/water. The product was separated by the Buchner funnel. The filtration was concentrated again. potassium cyamelurate $C_6N_7(OK)_3$ of the crystal was collected. (21 g, yield: 84 %).

(3) Synthesis of D

3.87 g C and 8.64 g PCl_5 was charged in a Schlenk bottle. The mixture was heated at 130 ^oC under vacuum for about two hours. 70 mL $POCl_3$ was added to the solid mixture and refluxed for 6 hours. The color of the reaction slurry turned from white to yellow. The solvent was removed and the residue solid was washed with cold water. (3.2 g, Yield:82%).

(4) Synthesis of E

3.6 g of 2,5,8-trichloro-*s*-heptazine (D) was dispersed in 40 mL of toluene. Anhydrate $AlCl_3$ was suspended in 40 mL of toluene and heated at 60 °C. To which solution of D was slowly added in batches. The color of the reactant changed to dark red once the 2,5,8-trichloro-*s*-heptazine was added. After reacted for 30 minutes, yellow compound can be observed. 300 mL of ice water was added. A large amount of yellow product appeared. The glassware was rinsed with THF. The product is filtered, and the solids were washed three times with acetone. (Yield of 2,5,8-*p*-methylbenzene-s-heptazine: 83 %). ^{1}H NMR, 2.017 (s, 9H), 7.024 (d, 6H), 8.854 (d, 6H).

(5) Synthesis of F

1 g of 2,5,8-*p*-methylbenzene-s-heptazine (E), 20.5 g HAc, 1.23 mL concentrated H_2SO_4 were added into a 100 mL flask in a 0 °C water bath. 2.03 g fine CrO_3 powder and 1.35 g Ac_2O was added slowly into the system. The flask was kept in the cool bath for 10 minutes. After that, the mixture was allowed to be stirred overnight. The color of solution was finally changed to green. The product was poured into 300 mL distilled water. The yellow solid was obtained by centrifugation and dissolved in 50 mL 6 M NaOH aqueous solution. Green solution and some white insoluble precipitate were obtained. After removing the precipitation by centrifugation, the solution was adjusted to pH 2, which gave rise to yellow precipitation. The solid was separated (by centrifugation) and washed successively by ethanol and ether (three times, 10 mL for each time), and then dried under vacuum (0.6 g, yield: 60 %). ^{1}H NMR, 8.17 (d 6H), 8.52 (d 6H) ,13.40 (s 3H).

2.2. Preparation of PFC-42 for single crystal x-ray diffraction analysis

H_3HTB (3 mg, 5.624 μmol) was dissolved in 5 mL methanol by sonication. The mixture stands at room temperature for 36 hours to afford yellow block crystals of PFC-42.

2.3. Synthesis of powdery PFC-42.

A mixture of H_3HTB (10mg, 0.01875mmol) and methanol (10.0 mL) were sealed in a 20 mL vial with silicone lined caps and heated at 90 ^{o}C for 24 h. After cooling to room temperature, the yellow powder was harvested and washed with methanol three times. (6.1 mg, yield: 61 %).

2.4. Synthesis of the bulk C_3N_4

The bulk C_3N_4 was prepared by thermal polymerization of melamine as previously reported.[2] Briefly, 5 g of melamine was placed into a corundum crucible and heated at 550 ^{o}C (ramp rate: 5 ^{o}C /min) under N_2 flow for 4 h (0.97g, yield: 19 %).

2.5. Synthesis of the nanosheets C_3N_4

C_3N_4 nanosheets were synthesized through thermal exfoliation of the protonated bulk C_3N_4.[2] In detail, bulk C_3N_4 powder was dispersed in a 0.7 M HNO_3 solution (1.0 g bulk C_3N_4 in 21.5 mL HNO_3) under stirring for 1 h to obtain protonated bulk C_3N_4. Then, the protonated bulk C_3N_4 was purified (by ultrasonic for 1 h), centrifuged, and rinsed with H_2O and EtOH. Finally, 1 g protonated bulk C_3N_4 was heated at 520 ^oC in air for 4 h (0.18 g, yield: 18 %).

2.6. Synthesis of powdery nanosheet C_3N_4-Pt

14 mg nanosheet C_3N_4 was dispersed in 10 mL of methanol by sonication. After that, 0.7 mL H_2PtCl_6 (1 mg/mL in methanol) was added into system, respectively. The solution w as sealed in a 20 mL vials and put into a preheated oven at 90 °C for 24 h

2.7. Synthesis of powdery PFC-42-Pt

PFC-42 (14 mg, 0.0073 mmol) was dispersed in 10 mL of methanol by sonication. After that, 0.4 mL, 0.7 mL and 1.2 mL H_2PtCl_6 (1 mg/mL in methanol) was added into system, respectively. The solution was sealed in a 20 mL vials and put into a preheated oven at 90 °C for 24 h.

2.8. Regeneration of PFC-42-Pt

The decomposed PFC-42-Pt (destroyed with 12M HCl) was dispersed in 10 mL MeOH. The mixture stands at 90 °C oven for 24 hours to afford regenerated yellow powder PFC-42-Pt.

2.9 Electrode preparation.

5 mg of PFC-42 was dispersed in 1 mL CH_3OH, with 50 μL 5% Nafion by ultrasonication for 0.5 h. The as-prepared solution was dropped on the surface of the fluorine-tin oxide (FTO) substrate covering an area about 1.0 × 1.0 cm^2 and then dried in air. This step was repeated three times to achieve uniform coverage. Other electrodes in this study were prepared following the same procedure.

2.10 Photoelectrochemical Measurements

Photoelectrochemical characterization was carried out in a standard three-electrode setup, with the Ag/AgCl (1 M KCl) as the reference electrode and a platinum plate as the counter electrode and fluorine-tin oxide (FTO) glass with the samples as the working electrode. 0.2 M $Na_2SO_4$was used as the electrolyte. An electrochemical workstation (CHI660D) was used to measure the photocurrent under visible-light illumination ($\lambda > 400$ nm, 350-W Xe lamp).

2.11 Photocatalytic Hydrogen Production Reaction

Photocatalytic hydrogen evolution was performed in a glass reaction cell with quartz cover connected with a closed gas circulation, and the entire system was purged with high purity Ar (99.999%) before illumination. 5 mg powdery samples were spread on the weighing bottle(50×30 mm) and then placed the bottle in the center of the reaction vessel. 13 mL deionized water and 2 mL TEOA were added below the sample holder avoiding direct contact with samples. After the entire system and water were completely degassed, 20 mL Ar was introduced into the system. This evacuation-refill operation was repeated 3 times prior to light irradiation. The visible-light irradiation was provided by a light-intensity-controlled xenon lamp (PerfectLight, Beijing) equipped with a UV-cut filter ($\lambda \geqslant 400$ nm). A cooling water-circulation system was used to keep the reaction system at room temperature. the gaseous products were analyzed online hourly using

an Agilent GC7820 gas chromatograph.

3. Characterizations

^{1}H-NMR spectra were recorded on Bruker AVANCE III 400MHz spectrometers. Single-crystal X-ray diffraction data were collected at 100 K on an Oxford Diffraction SuperNova diffractometer equipped with Cu-Kα radiation (λ=1.5418 Å). PXRD was performed on Rikagu Miniflex 600 Benchtop X-ray diffraction instrument. TGA was performed on a Seiko S-II instrument, and the dried crystalline samples were heated at a rate of 5 °C/min up to 800 °C and then cooled to room temperature under N_2 atmosphere. CO_2 adsorption-desorption isotherms were performed on Micromatic ASAP 2020 at 273 K. Inductively coupled plasma mass spectrometry (ICP-MS) was conducted on Ultima 2 Inductively Coupled Plasma OES spectrometers from Elementary. The morphology observations were carried on (a HITACHI SU8000 field-emission scanning electron microscope) JSM6700 scanning electron microscopy (SEM), JEM2010 transmission electron microscopy (TEM). UV-vis diffuse reflectance spectra (DRS) were recorded using a UV-vis spectrophotometer (Shimadzu UV-2550) equipped with an integrating sphere, and $BaSO_4$ powder was used as the reference for the baseline correction. Fourier transform infrared spectroscopy (FTIR) spectra were obtained on a Bruker Spectrum in the range of 4000–250 cm^{-1}. X-ray photoelectron spectroscopy (XPS) measurements were performed with the use of an ESCALAB 250Xi spectrometer equipped with an Al-Kα X-ray source (1486.6 eV). The solid-state fluorescent spectra were measured at room temperature on an Edinburgh-instruments FS5 fluorescence spectrophotometer. fluorescence quantum efficiency were measured at room temperature on an Edinburgh-instruments FS5 fluorescence spectrophotometer with integrating sphere accessory. The electrochemical impedance spectra (EIS), photocurrent response, and Mott-Schottky plots were carried out on IM6ex (Zahner, Germany).

4. Single-Crystal X-ray Crystallography of PFC-42

Single-crystal X-ray diffraction data were collected at 100 K on an Oxford Diffraction SuperNova diffractometer equipped with Cu-Kα radiation (λ = 1.54184). The cell refinement and data collection and reduction are solved by CrysAlisPro software package. The structure was solved by direct method and refined using Olex 2 and SHELXL-2016 software package.

Table.S1 Crystal data and structure refinement results for PFC-42.

Empirical formula	$C_{27}H_{15}N_7O_6$
Formula weight	533.46
Temperature/K	100
Crystal system	monoclinic
Space group	$P2_1/n$
a/Å	7.5193(4)
b/Å	19.0692(9)
c/Å	20.4491(8)
α/°	90
β/°	99.627(4)

γ/°	90
Volume/Å^3	2890.8(2)
Z	4
ρ_{calc}g/cm^3	1.219
μ/mm^{-1}	0.757
F(000)	1084.0
Radiation	Cu Kα (λ = 1.54184)
2Θrange for data collection/°	4.386 to 74.040
Index ranges	-9 ≤ h ≤ 7, -21 ≤ k ≤ 23, -25 ≤ l ≤ 23
Reflections collected	11613
Independent reflections	5643 [R_{int} = 0.0318, R_{sigma} = 0.0381]
Data/restraints/parameters	5643/0/328
Goodness-of-fit on F^2	1.137
Final R indexes [I>=2σ (I)]	R_1 = 0.1032, wR_2 = 0.3024
Final R indexes [all data]	R_1 = 0.1442, wR_2 = 0.3267
Largest diff. peak/hole / e Å^{-3}	1.344/-0.756

5. Supplementary Figures

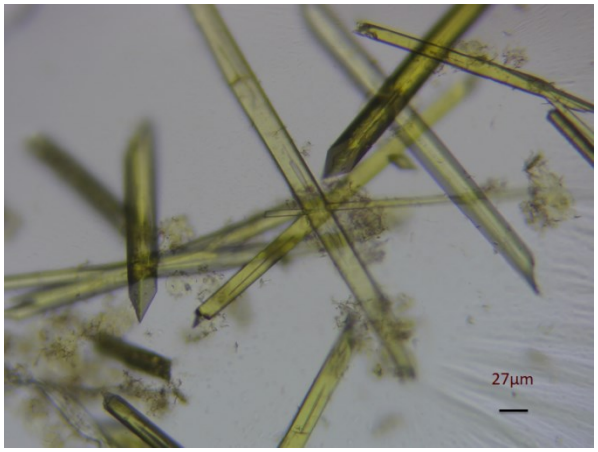

Figure S1. The microscope image of PFC-42.

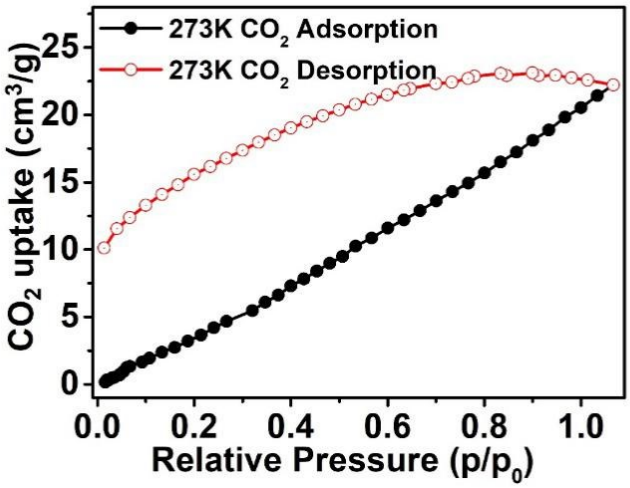

Figure S2. CO_2 adsorption isotherm of PFC-42 at 273 K.

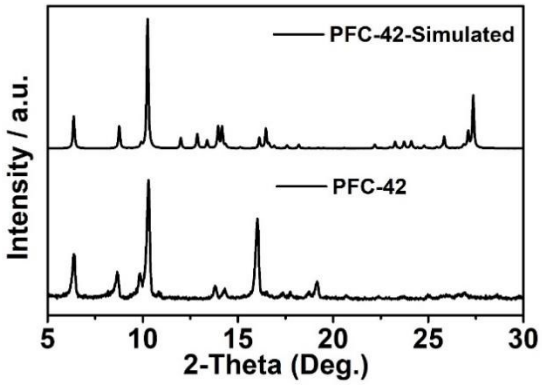

Figure S3. PXRD patterns of the as-synthesized and simulated PFC-42.

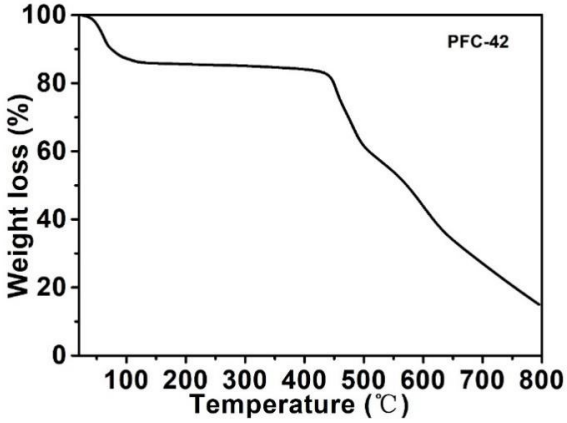

Figure S4. TGA curves of as-synthesized PFC-42.

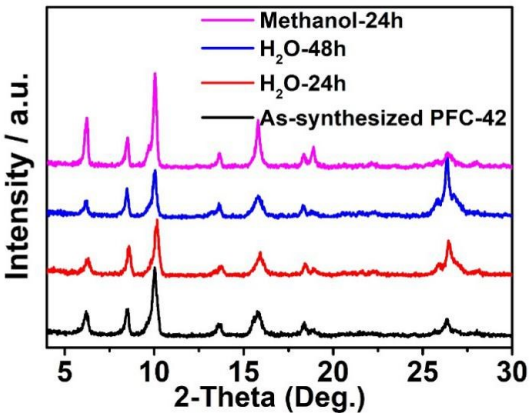

Figure S5. PFC-42 after being immersed in different solvents.

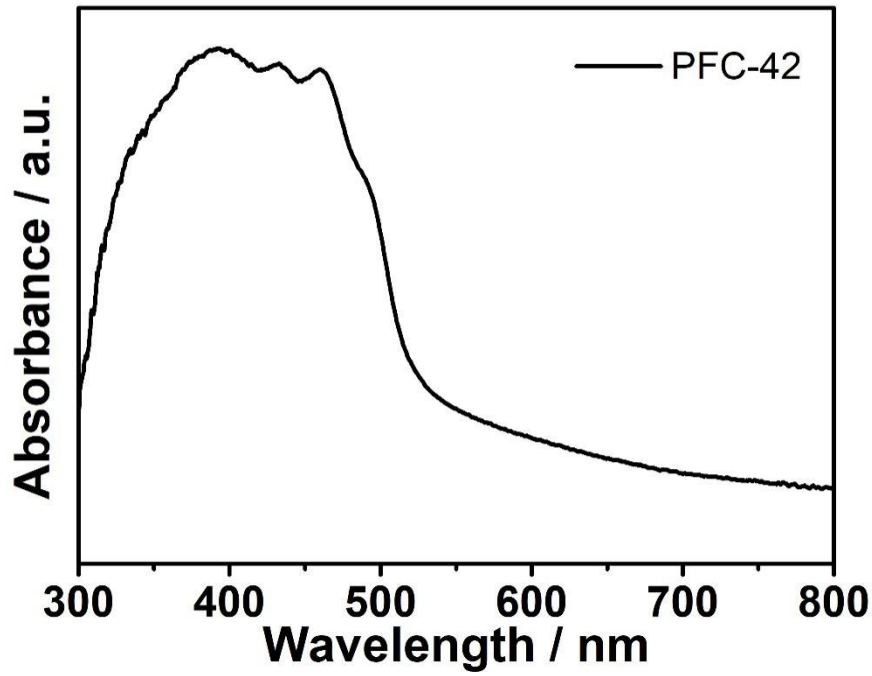

Figure S6. UV/vis diffuse reflectance spectra of PFC-42.

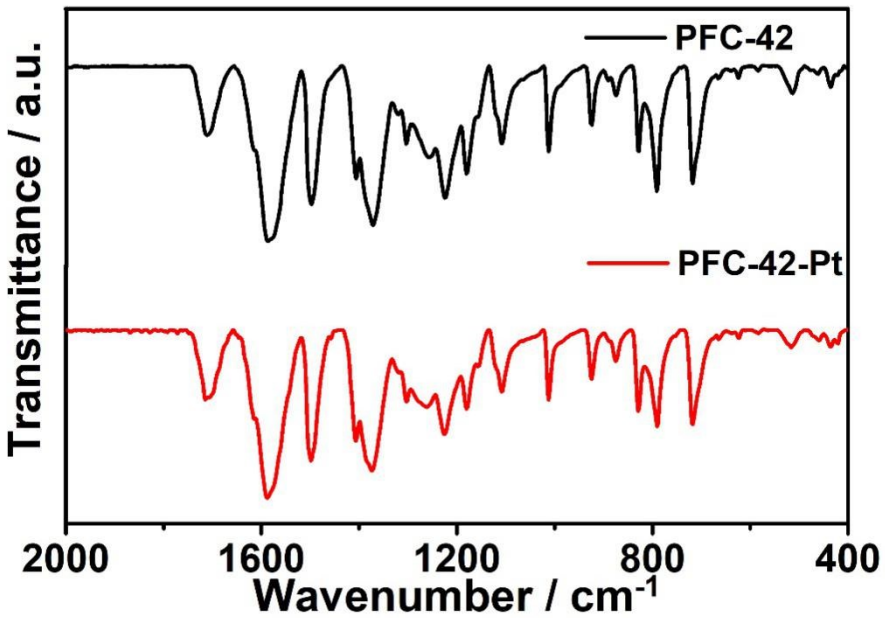

Figure S7. ATR-IR spectra of PFC-42 before and after loading PtNP.

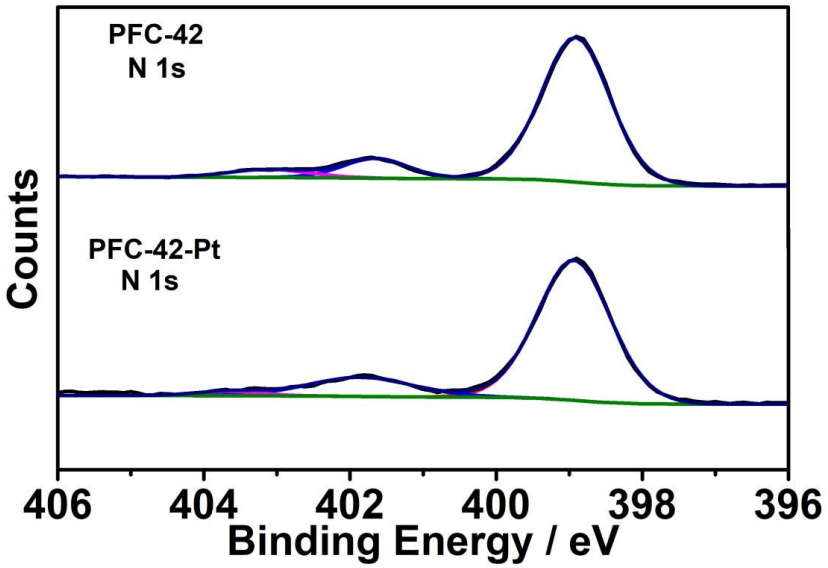

Figure S8. Comparison of XPS spectra of N 1*s* orbitals of PFC-42 and PFC-42-Pt.

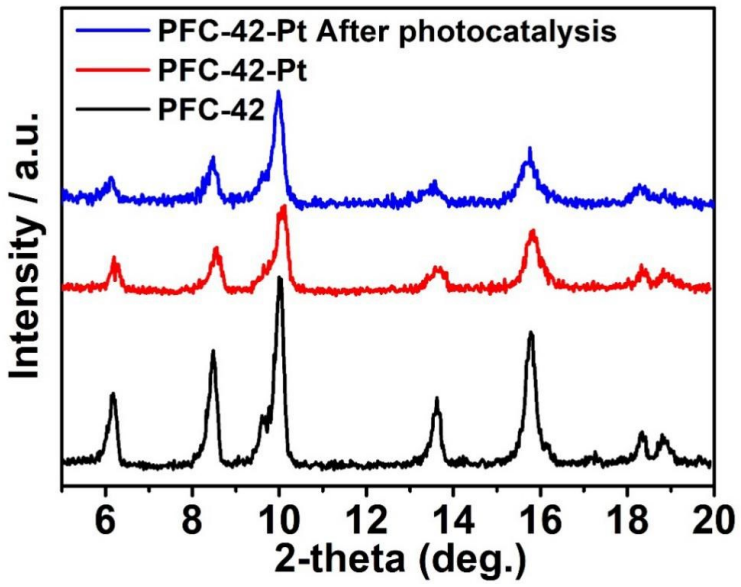

Figure S9. PXRD patterns of as-synthesized PFC-42, PFC-42-Pt, and PFC-42-Pt after photocatalysis.

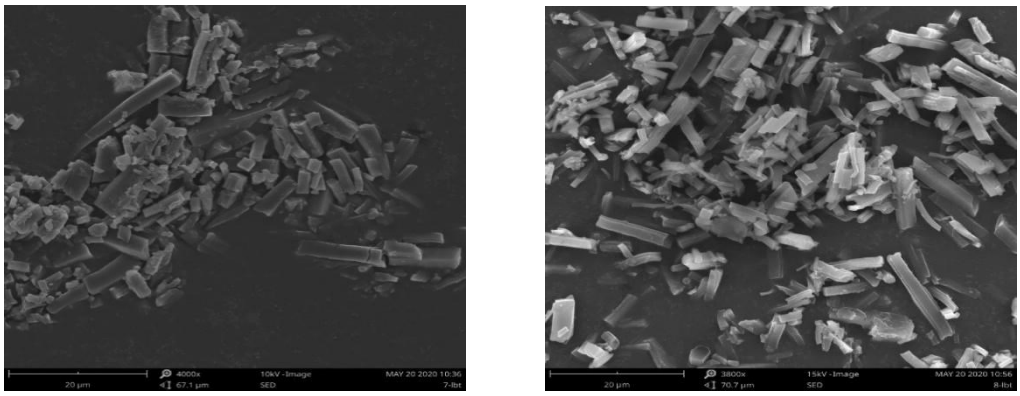

Figure S10. SEM images of PFC-42 before and after loading Pt.

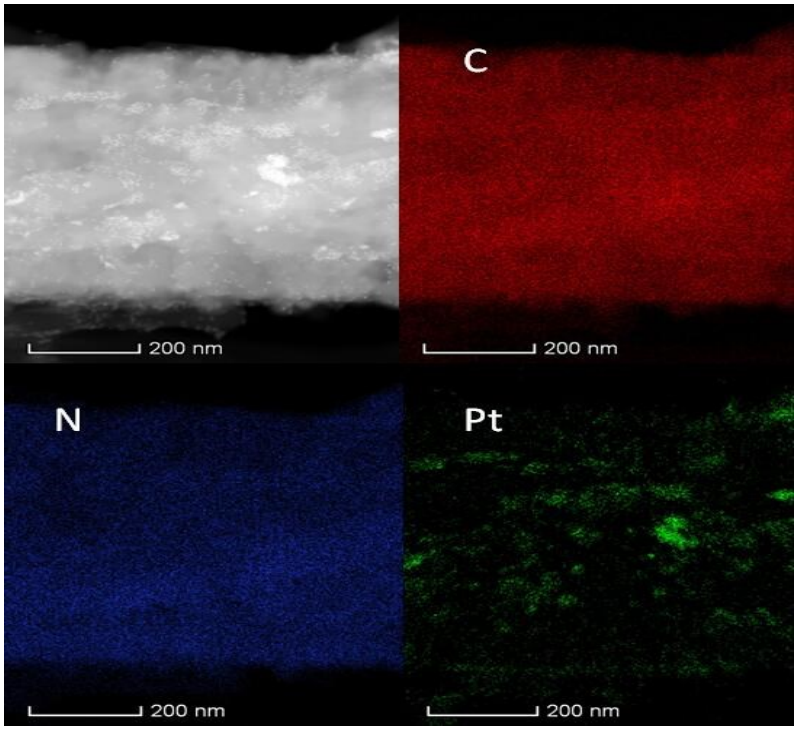

Figure S11. Elemental mapping of PFC-42-Pt.

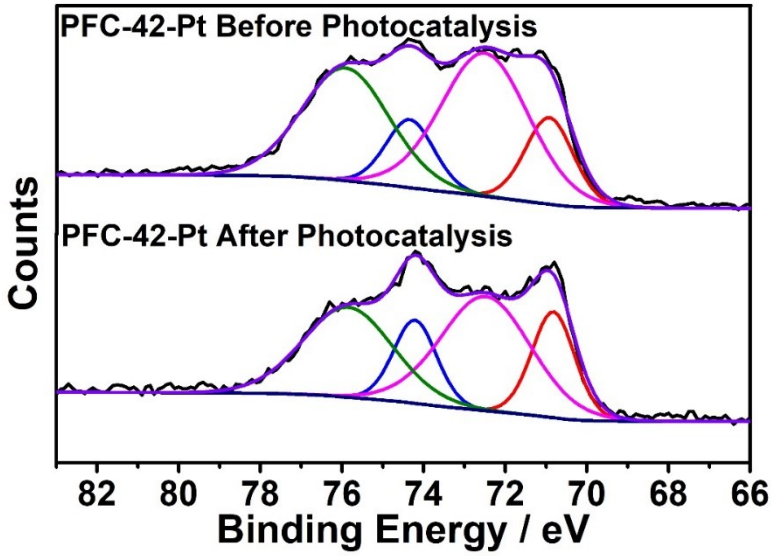

Figure S12. Pt 4f XPS spectra of PFC-42 before and after H_2 evolution.

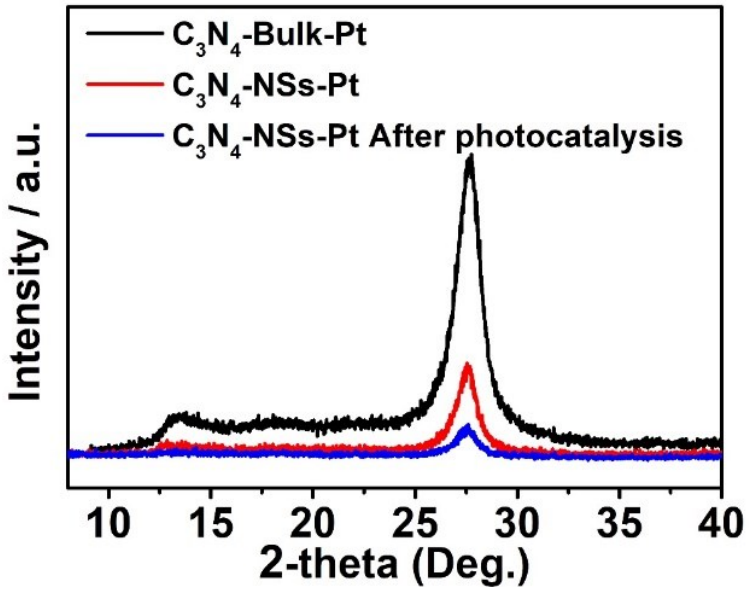

Figure S13. PXRD patterns of as-synthesized bulk C_3N_4-Pt, nanosheet C_3N_4-Pt, and C_3N_4-Pt after photocatalysis.

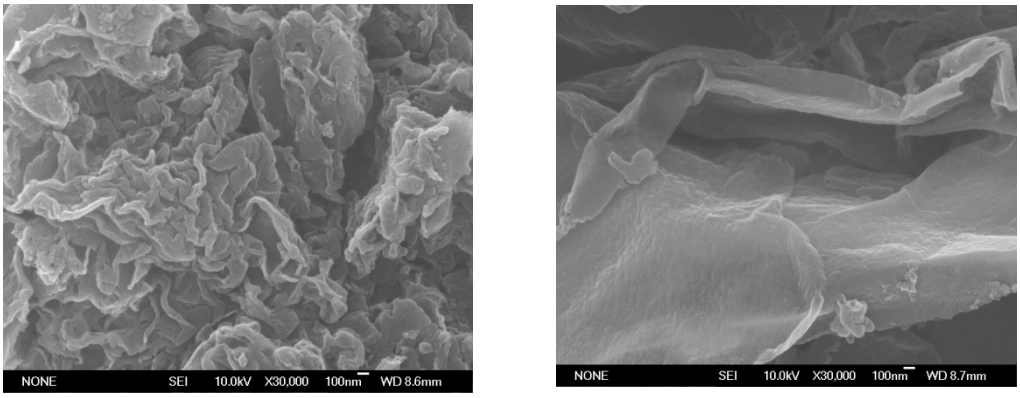

Figure S14. SEM images of nanosheet C_3N_4

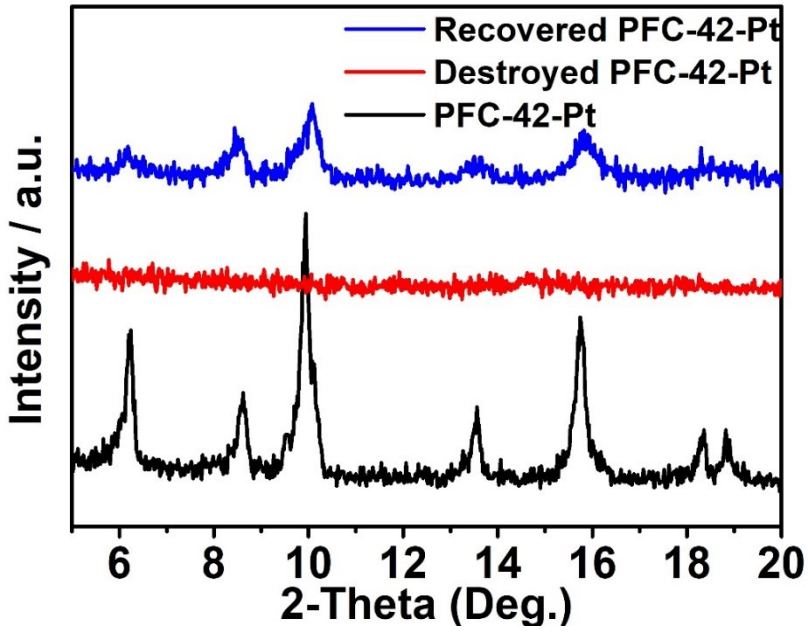

Figure S15. PXRD patterns of as-synthesized PFC-42-Pt, PFC-42-Pt-decomposed (destroyed with 12M HCl), and recovered PFC-42-Pt.

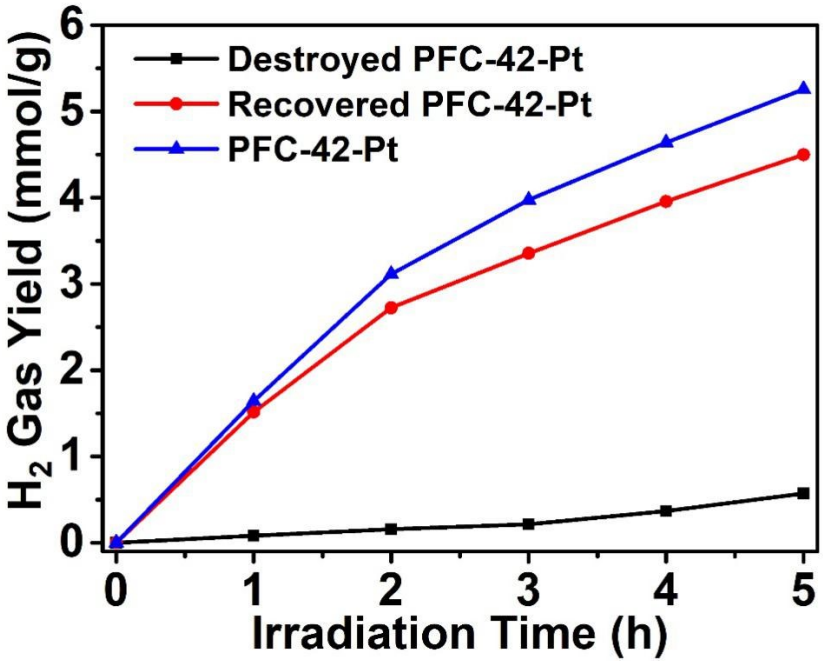

Figure S16. Photocatalytic H_2 evolution performance of as-synthesized PFC-42-Pt, Destroyed PFC-42-Pt (destroyed with 12M HCl), and-Recovered PFC-42-Pt (immersed in Methanol for 24h).

Table S2. The apparent quantum efficiency results for PFC-42.

Wavelength (nm)	Irradiance (W * π cm^{-2})	H_2–evolution (μmol h^{-1} 5mg^{-1})	AQY (%)
λ=420	0.47	26.4	5.56

AQY is defined as the ratio of the number of reacted electrons to the number of incident photons. The general equation is given below:

$$AQY\ (\%) = \frac{2 \times the\ number\ of\ evolved\ hydrogen\ molecules}{the\ number\ of\ incident\ photons} \times 100$$

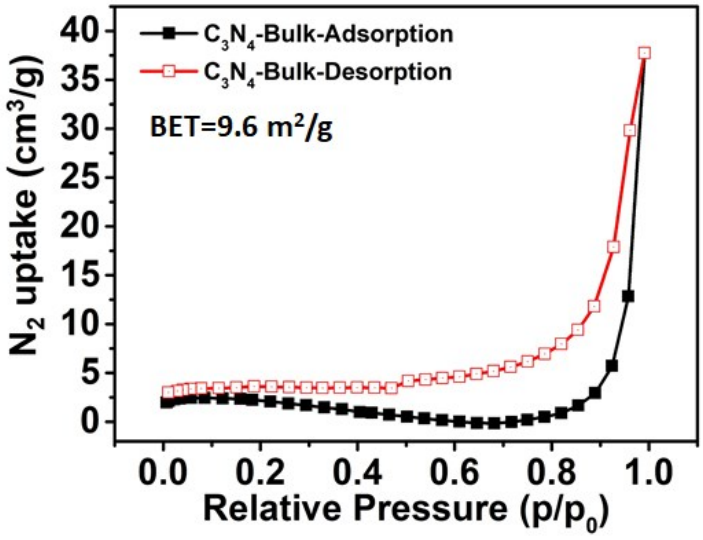

Figure S17. N_2 adsorption isotherm of bulk C_3N_4 at 77 K.

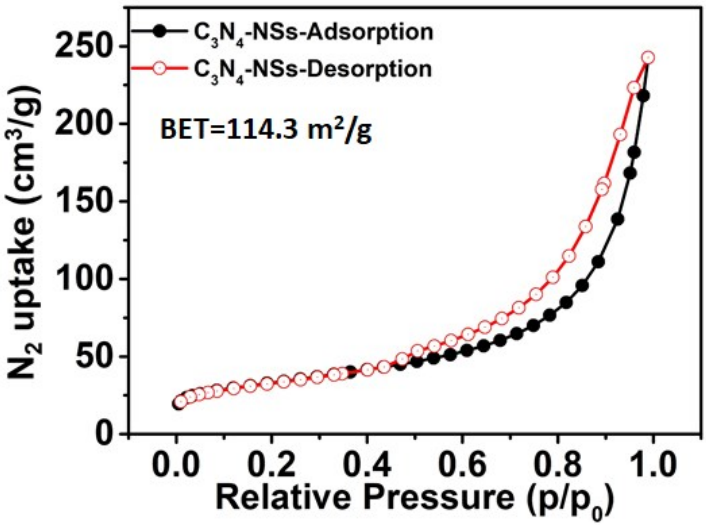

Figure S18. N_2 adsorption isotherm of nanosheet C_3N_4 at 77 K.

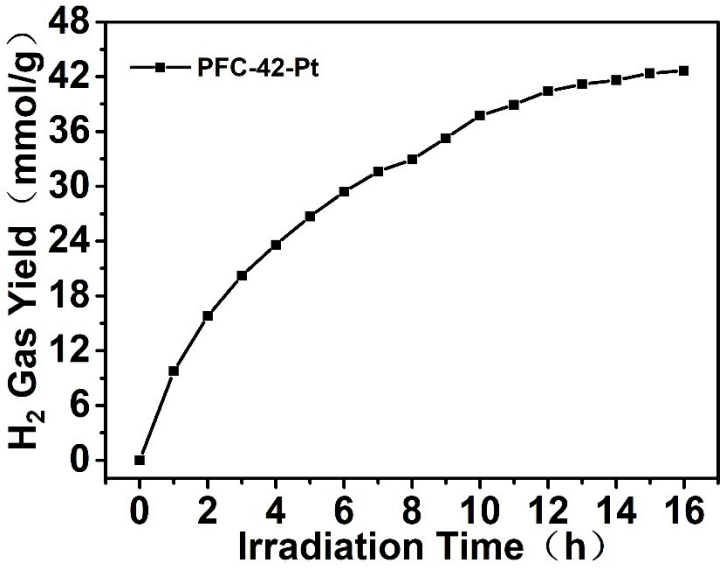

Figure S19. Photocatalytic activity lasting 16 hours.

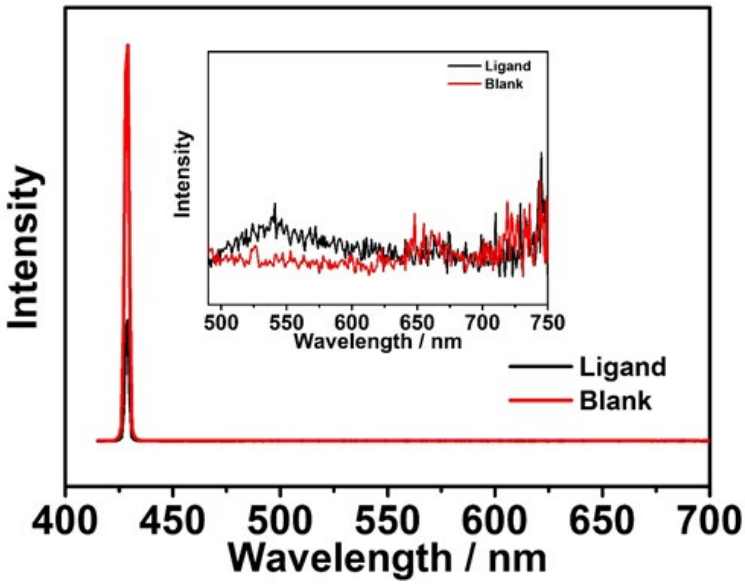

Figure S20. Fluorescence quantum efficiency of ligand.

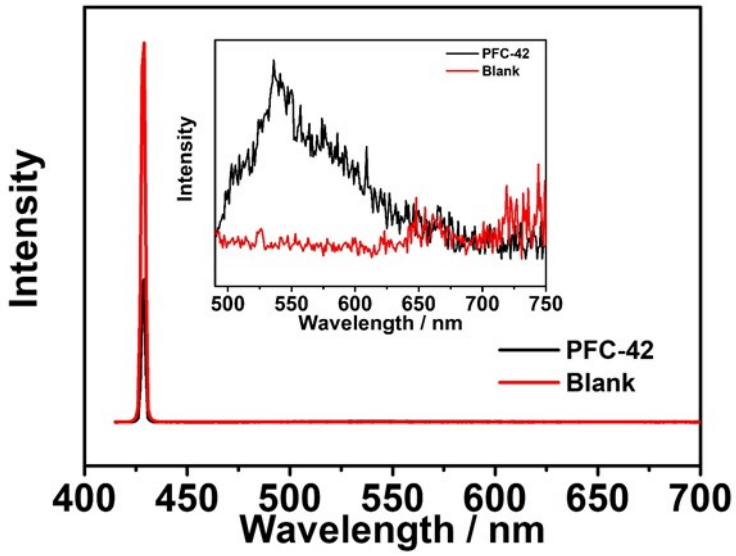

Figure S21. Fluorescence quantum efficiency of PFC-42.

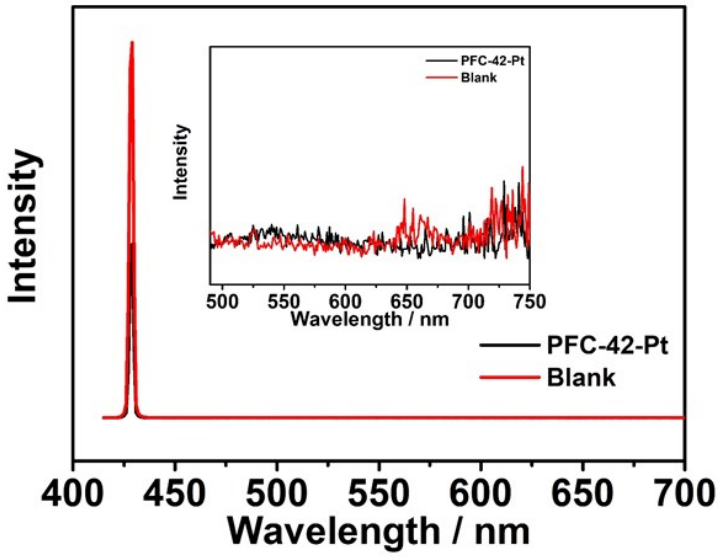

Figure S22. Fluorescence quantum efficiency of PFC-42-Pt.

Table S3. Fluorescence quantum efficiency results.

	FigureS20 Ligand	**FigureS21** PFC-42	**Figure S22** PFC-42-Pt
Fluorescence quantum efficiency	1.30%	7.80%	0.527%

All the samples are dispersed in ultrapure water with the same mass. Ultrapure water was used as a blank sample.

6. Summary of the performance of similar catalytic systems

Table S4. Summary of the activities of similar MOF or COF-based photocatalysts for H_2 evolution.

Photocatalyst	Cocatalyst	Electron donor	Solvent	Illumination	Activity ($\mu mol\ g^{-1}\ h^{-1}$)	420nmAQY (%)	Ref
PFC-42-Pt	**Pt**	**TEOA**	**H_2O**	**> 400 nm**	**9733**	**5.56**	**This work**
Pt/x%-MIL-125-$(SCH_3)_2$	Pt	TEOA	H_2O	> 400 nm	3814	**8.90**	[3]
TFPT-COF	Pt	TEOA	H_2O	> 420 nm	1970	**2.20**	[4]
Pt@MIL-125/Au	Pt&Au	TEOA	CH_3CN/ H_2O	380-800 nm	1743	–	[5]
N_3-COF	Pt	TEOA	PBS Buffer	> 420 nm	1703	–	[6]
sp^2c-COF	Pt	TEOA	H_2O	> 420 nm	1360	**0.46**	[7]
Pt/PCN-777	Pt	TEOA	DMF/ H_2O	AM 1.5G	586	–	[8]
USTC-8(In)	Pt	TEA	CH_3CN/ H_2O	> 380 nm	341.3	–	[9]
TP-BDDA	Pt	TEOA	H_2O	≥ 395 nm	324	**1.30**	[10]
Pt@UiO-66-NH_2	Pt	TEOA	CH_3CN/ H_2O	> 380 nm	257.38	–	[11]
Al-TCPP-0.1Pt	Pt	TEOA	CH_3CN/ H_2O	> 420 nm	129	–	[12]
Pt/Cd-TBAPy	Pt	TEOA	CH_3CN/ H_2O	> 420 nm	86	–	[13]

7. References:

(1) Ke, Y. X.; Collins, D. J.; Sun, D. F.; Zhou, H. C. (10,3)-a noninterpenetrated network built from a Piedfort ligand pair. *Inorg Chem.* **2006**, *45*, 1897-1899.

(2) Li, J.; Chen, Y.; Yang, X.; Gao, S.; Cao, R. Visible-light-mediated high-efficiency catalytic oxidation of sulfides using wrinkled C_3N_4 nanosheets. *J Catal.* **2020**, *381*, 579-589.

(3) Han, S.-Y.; Pan, D.-L.; Chen, H.; Bu, X.-B.; Gao, Y.-X.; Gao, H.; Tian, Y.; Li, G.-S.; Wang, G.; Cao, S.-L.; Wan, C.-Q.; Guo, G.-C. A Methylthio-Functionalized-MOF Photocatalyst with High Performance for Visible-Light-Driven H-2 Evolution. *Angew. Chem., Int. Ed*. **2018**, *57*, 9864-9869.

(4) Stegbauer, L.; Schwinghammer, K.; Lotsch, B. V. A hydrazone-based covalent organic framework for photocatalytic hydrogen production. *Chem Sci.* **2014**, *5*, 2789-2793.

(5) Xiao, J.-D.; Han, L.; Luo, J.; Yu, S.-H.; Jiang, H.-L. Integration of Plasmonic Effects and Schottky Junctions into Metal-Organic Framework Composites: Steering Charge Flow for Enhanced Visible-Light Photocatalysis. *Angew. Chem. Int. Ed*. **2018**, *57*, 1103-1107.

(6) Vyas, V. S.; Haase, F.; Stegbauer, L.; Savasci, G.; Podjaski, F.; Ochsenfeld, C.; Lotsch, B. V. A tunable azine covalent organic framework platform for visible light-induced hydrogen generation. *Nat Commun.* **2015**, *6*, 8508.

(7) Jin, E.; Lan, Z.;Jiang, Q.; Geng, K.; Li, G.; Wang, X.; Jiang, D. 2D sp^2 Carbon-Conjugated Covalent Organic Frameworks for Photocatalytic Hydrogen Production from Water. *Chem.***2019**, *5(6)*, 1632-1647.

(8) Liu, H.; Xu, C.; Li, D.; Jiang, H.-L. Photocatalytic Hydrogen Production Coupled with Selective Benzylamine Oxidation over MOF Composites. *Angew. Chem. Int. Ed.* **2018**, *57*, 5379-5383.

(9) Leng, F.; Liu, H.; Ding, M.; Lin, Q.-P.; Jiang, H.-L. Boosting Photocatalytic Hydrogen Production of Porphyrinic MOFs: The Metal Location in Metalloporphyrin Matters. *Acs Catal.* **2018**, *8*, 4583-4590.

(10) Pachfule, P.; Acharjya, A.; Roeser, J.; Langenhahn, T.; Schwarze, M.; Schomaecker, R.; Thomas, A.; Schmidt, J. Diacetylene Functionalized Covalent Organic Framework (COF) for Photocatalytic Hydrogen Generation. *J Am Chem Soc.* **2018**, *140*, 1423-1427.

(11) Xiao, J.-D.; Shang, Q.; Xiong, Y.; Zhang, Q.; Luo, Y.; Yu, S.-H.; Jiang, H.-L. Boosting Photocatalytic Hydrogen Production of a Metal-Organic Framework Decorated with Platinum Nanoparticles: The Platinum Location Matters. *Angew. Chem. Int. Ed.* **2016**, *55*, 9389-9393.

(12) Fang, X.; Shang, Q.; Wang, Y.; Jiao, L.; Yao, T.; Li, Y.; Zhang, Q.; Luo, Y.; Jiang, H.-L. Single Pt Atoms Confined into a Metal-Organic Framework for Efficient Photocatalysis. *Adv Mater.* **2018**, *30(7):*1705112.

(13) Xiao, Y.; Qi, Y.; Wang, X.; Wang, X.; Zhang, F.; Li, C. Visible-Light-Responsive 2D Cadmium-Organic Framework Single Crystals with Dual Functions of Water Reduction and Oxidation. *Adv Mater.* **2018**, *30(44)*:1803401.1-1803401.7.